Int. J. Nanoelectronics and Materials **9** (2016) 1-8

Influence of Co-doping on the Structural, Optical and Magnetic Properties of ZnO Nanoparticles

Raminder Preet Pal Singh[1,*], I.S. Hudiara[2], Sudhakar Panday[3], Pushpendra Kumar[4], S. B. Rana[5]

[1,3]*Department of Electronics & Communication Engineering, Desh Bhagat University, Mandi Gobindgarh, India*
[2]*Chitkara University (Punjab Campus), Chandigarh, India*
[4]*Department of Chemistry, Arni University, Kangra, Himachal Pradesh, India.*
[5]*Department of ECE, GNDU, Regional Campus, Gurdaspur.*

Received 23 April 2015; Revised 25 June 2015; Accepted 7 July 2015

Abstract

In this study, undoped ZnO and Co-doped ZnO ($Zn_{1-x}Co_xO$ (x=0, 0.01, 0.03 and 0.05)) diluted magnetic semiconductor (DMS) nanoparticles were synthesized using co-precipitation method. The structural, optical and magnetic properties of the Co-doped ZnO samples annealed at 600^oC were characterized by X-ray diffractometer (XRD), Scanning electron microscope (SEM), UV-visible absorption spectroscopy and Vibrating sample magnetometer (VSM). The average crystalline size was calculated using Debye-Scherrer's formula. The particle size was found to be in the range of 39 to 50 nm. The X-ray diffraction studies revealed that the synthesized Co doped ZnO nanoparticles have single phase wurtzite structure with no signature of secondary phases. However, the position of diffracted peaks slightly shifted towards lower (2θ) angles. SEM micro-image confirmed the presence of spherical $Zn_{1-x}Co_xO$ nanoparticles. VSM measurements show the hysteresis loop with high coercive value at room temperature which confirms the ferromagnetic property of the samples. The presence of ferromagnetic behavior is due to intrinsic coupling among the atoms of doped materials.

Keywords: $Zn_{1-x}Co_xO$ nanoparticles, Co-doping, diluted magnetic semiconductor, magnetic properties, Spintronics, UV-visible absorption spectroscopy.
PACS: 81.05.Dz, 75.75.Fk, 07.60.Rd, 75.50.Cc, 75.50.Lk, 75.50.-y

1. Introduction

ZnO is a group II-IV semiconductor and has become one of the most promising candidates for DMS materials. Moreover, ZnO has potential applications in optoelectronics due to its wide band-gap (3.3 eV) and high exciton binding energy (60 meV) properties [1-4].

DMS are semiconductor materials in which a fraction of host cations can be easily

*) For Correspondence, E-mail: raminder_212003@rediffmail.com

replaced by magnetic ions in order to achieve controlled conduction and high degree of spin polarization. Scientists are investigating the effect of doping ZnO with transition metals such as Fe, Mn and Ni [9-16]. A number of experiments have been carried out to investigate the structural and magnetic properties of Co-doped ZnO [17-22]. Experimental studies confirm that ferromagnetism strongly depends on synthesis techniques and environmental conditions used for the preparation of samples. Various chemical methods have been developed to prepare nanoparticles of different materials of interest. Most ZnO nanocrystals have been synthesized by traditional high temperature solid state reaction method. However this method is time consuming and properties of the product can't be controlled. ZnO nanoparticles can be prepared on a large scale at low cost by simple solution based methods, such as chemical co-precipitation, hydrothermal reaction, and sol-gel synthesis.

In this work, we synthesized $Zn_{1-x}Co_xO$ nanoparticles using co-precipitation method. This is a simple and low cost method which gives a good end product yield and is less time consuming. In this research work we studied the effect of dopant ion concentration on the structure and magnetic properties of Co doped ZnO ($Zn_{1-x}Co_xO$ (x = 0.01, 0.03 and 0.05) annealed at 600^0C.

2. Experiment

Pure ZnO nanoparticles and Co doped ZnO diluted magnetic semiconductors nanoparticles were synthesized by co-precipitation method. Zinc Acetate ($Zn(CH_3COO)_2 .2H_2O$) and Cobalt Acetate ($Co(C_2H_3O_2)_2 .4H_2O$) were chosen according to the calculated stoichiometric ratio in a beaker containing 100 ml distilled water and stirred for 1h. NaOH mixed in distilled water was added drop by drop to the solution till the PH value of solution reached 10. The solution was then stirred at room temperature for 2 h followed by aging for 24 hrs at the same temperature. After aging, precipitate that formed was filtered. The product obtained at this stage was Zinc and Cobalt hydroxide powder. Finally, thermal decomposition of the Zinc and Cobalt hydroxide was done to obtain $Zn_{1-x}Co_xO$ nanocrystals. For that, samples were annealed at 600°C for 2 h.

3. Results and Discussion

An X-ray diffraction patterns of powder samples were recorded by glancing angle X-ray diffractometer (Bruker AXS D8 Advance, Germany), to investigate the phase formation and the effect of Co incorporation. The diffractometer was equipped with graphite monochromator, a mirror at a fixed incidence angle of 1-5° and CuKα as the radiation source. The angular accuracy was 0.001° and the angular resolution was better than 0.01°. For study of surface morphology, scanning electron microscope Carl Zeiss Supras 55 was used. A Microsense E29 Vibrating Sample Magnetometer (VSM) was used to study the magnetic properties (M-H Curve) at room temperature of the synthesized samples.

4. Results and discussions

4.1 XRD Analysis

X-ray diffraction patterns of Co doped ZnO showed exhaustive evolution of hexagonal wurtzite phase in all the samples and no other secondary and impurity phase was detected. Overall the samples' peak intensity was very high which confirmed good crystalline formation. Figure 1, shows this with increase in cobalt doping concentration.

Intensity of the peaks decreased compared to undoped ZnO, which revealed incorporation of cobalt dopant into the ZnO wurtzite lattice as a substitute atom.
It has been reported in the literature that when a foreign particle is incorporated in the crystal lattice, it produces a strain and defect(s) in the lattice which may reduce the crystal quality [23].

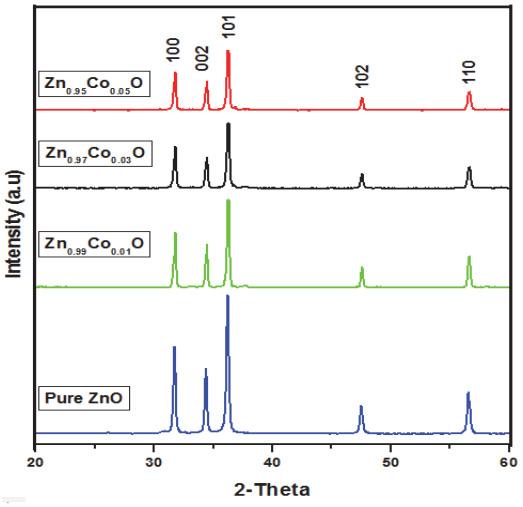

Fig. 1: XRD patterns of pure ZnO and $Zn_{1-x}Co_xO$ (x = 0.01, 0.03, and 0.05) nanoparticles annealed at 600℃.

However, an insight analysis of the position of the XRD peak (as shown in figure 2), indicates very minute shifting of peak toward lower 2θ value with an increase in cobalt doping. The change in the peak positions i.e. peak 102 clearly indicates that Co ions are occupying the Zn position in the ZnO matrix [24].

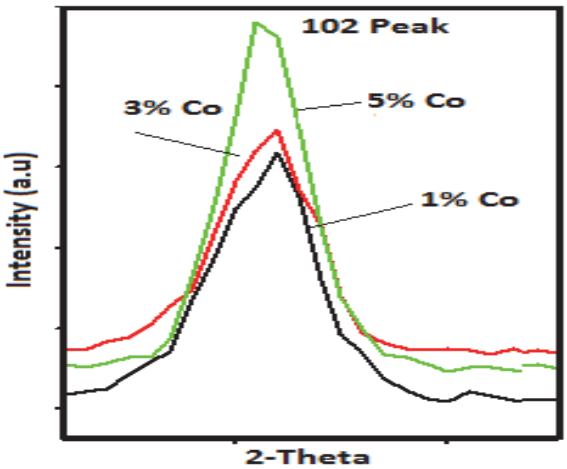

Fig. 2: Shifting of (102) peak with the doping concentration of $Zn_{1-x}Co_xO$ samples annealed at 600℃.

In doping, ionic radii plays an important role. If the ionic radii of foreign particle are higher or lower than the host lattice, then lattice parameters of host expand or contract to accommodate it. The lattice parameters calculated (as shown in table 1) from the XRD data show that their values are nearly equal to pure ZnO. Moreover, it is evident that the variation of the lattice parameters with respect to Co concentration is not monotonic. The main reason behind this is the closeness of effective ionic radius (0.58 Å) of Co^{2+} in tetrahedral configuration to that of Zn^{2+} (0.60 Å) [25-26]. The average crystalline size was

calculated by using scherrer's equation (1) and was found to be in the range of 39 nm to 50 nm as shown in table 1.

$$\tau = \frac{k\,\lambda}{B\,\mathrm{Cos}\,\theta} \qquad (1)$$

where, τ is grain size, B is the full width at half maxima and λ is the wavelength of X-ray used (1.548 Å) and θ is the diffraction angle. The values of lattice strain are also shown in table 1 and are very low. The lattice parameters were calculated using equation (2) given below.

$$\frac{1}{d^2} = \frac{4}{3}\left[\frac{h^2 + hk + k^2}{a^2}\right] + \frac{l^2}{c^2} \qquad (2)$$

Where d, h, *l*, k, a and c are lattice constants.
The calculated values shown in table 1 are very close to the reported values in literature [25].

Table 1: Lattice and Optical Parameters of pure ZnO and Co-doped nanoparticles annealed at 600℃.

Co Doping %	Scherrer Size	Lattice Strain	d_{101} (Å) Spacing	Unit Cell Parameters		c/a ratio	Dislocation Density (10^{-3}) linem^{-2}	Absorption Wavelength (λ)	Band Gap Energy (Eg)
				a	c				
0 %	39.0 nm	0.0027	2.4755	3.232	5.278	1.6330	0.65	380 nm	3.27
1%	40.0 nm	0.0021	2.4749	3.2316	5.2769	1.6329	0.4	383 nm	3.24
3%	42.7 nm	0.0025	2.4752	3.2320	5.2775	1.6329	0.54	385 nm	3.22
5%	44.3 nm	0.0024	2.4755	3.2324	5.2781	1.6328	0.51	388 nm	3.20

4.2 Scanning Electron Microscope (SEM) Analysis

Figure 3(a-d) shows SEM images of pure ZnO, $Zn_{0.99}Co_{0.01}O$, $Zn_{0.97}Co_{0.03}O$ and $Zn_{0.95}Co_{0.05}O$ i.e Co doped ZnO nanoparticles (1%, 3% and 5%) with an average particle size of approximately 65 nm, 66 nm, 68 nm and 70 nm respectively. The SEM images, confirmed that as synthesized material is in nano range and in good agreement with calculated crystalline size from XRD. The particle size measured from XRD is quite different from the SEM measurement because in SEM calculation is done by taking the difference of noticeable grain boundaries, whereas in case of XRD measurements are taken from the crystalline area that reasonably diffracts the X-ray waves. Figure 3(a) shows the SEM images of pure ZnO nanoparticles with spherical shape & large aggregation. However, it is clearly found from the figure 3 (b-d), the presence of Co-doped ZnO (1% to 5%) nanoparticles with large size distributions. Hence, for doped ZnO (1% to 5%) the less porocity is clearly seen in background with homogeneous grain distribution of dopant on increasing the dopant concentration. The SEM images shows all the nanocrystals having clear grain boundaries and close to the haxagonal shape. Incorporation of Co in ZnO matrix was further confirmed by EDAX analysis as highlighted in table 2. The estimated values of Co in ZnO are shown in table 2, which indicates that % age of Co incorporated in the samples is lower than their actual composition incorporated during the synthesis process.

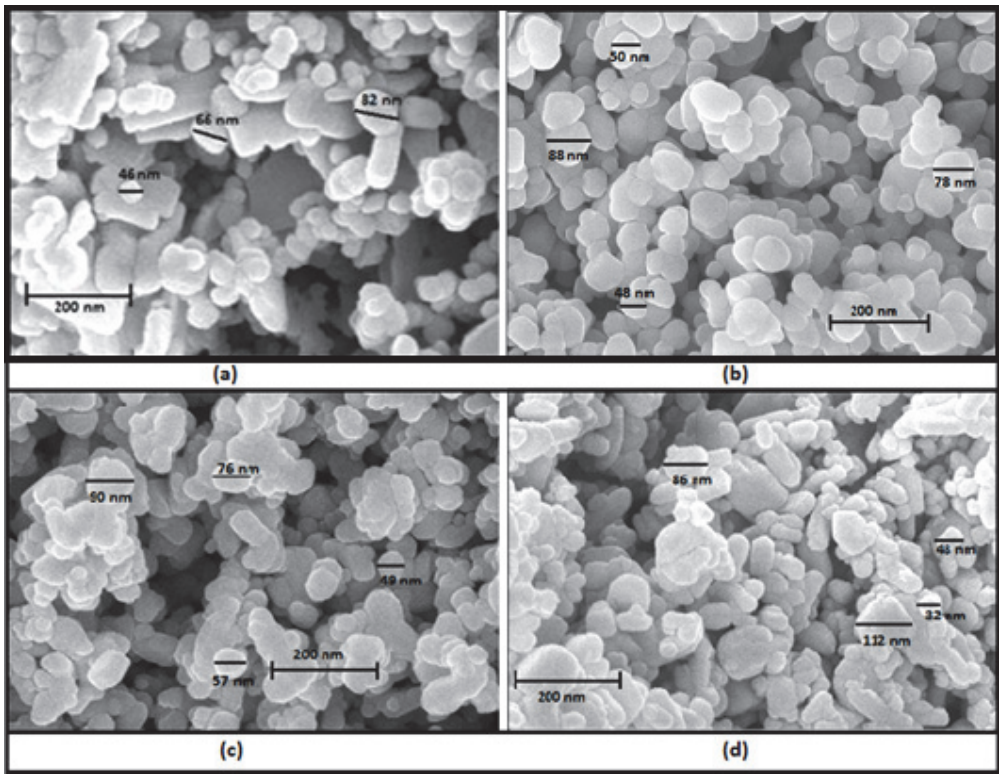

Fig. 3: SEM image of (a) Pure ZnO (b) $Zn_{0.99}Co_{0.01}O$ (c) $Zn_{0.97}Co_{0.03}O$ and (d) $Zn_{0.95}Co_{0.05}O$ nanoparticles

Table 2: EDAX data of Co-doped ZnO nanoparticle.

Sample	Co %	Zn %	O %
$Zn_{0.99}Co_{0.01}O$	0.59	48.71	50.70
$Zn_{0.97}Co_{0.03}O$	1.86	52.98	45.16
$Zn_{0.95}Co_{0.05}O$	2.51	48.08	49.41

4.3 Optical Absorption Study

Undoped and Co-doped ZnO nanoparticles were compared using UV-Visible absorption spectroscopy. Figure 4(a), shows the absorption spectra of the undoped ZnO nanoparticles with the absorption peak around 380 nm. We know from literature that the band gap wavelength of 377 nm (Eg= 3.28 eV) corresponds to the bulk ZnO nanoparticles [26].

Figure 4(b), shows the UV-Visible absorption spectra of the Co-doped ZnO nanoparticles with the absorption spectra for a wavelength range from 383 nm to 388 nm at different Co doping concentrations. Table 1, summarizes the band gap energy (Eg) for undoped and Co doped ZnO nanoparticles for different doping concentrations. From table 1, it is concluded that band gap energy decreases with the increase in doping concentration, which shows a small red shift. The decrease in band gap is due to an increase in the particle size with the increase in doping concentration and also due to *sp-d* exchange interaction among ZnO band and localized *d*-electrons of the substituted Co^{2+} cation [20]. Continuous

broadening of absorption peak with increase in Co-doping as observed from the figure, further clarifies that size of nanocrystals increase with an increase in doping concentration.

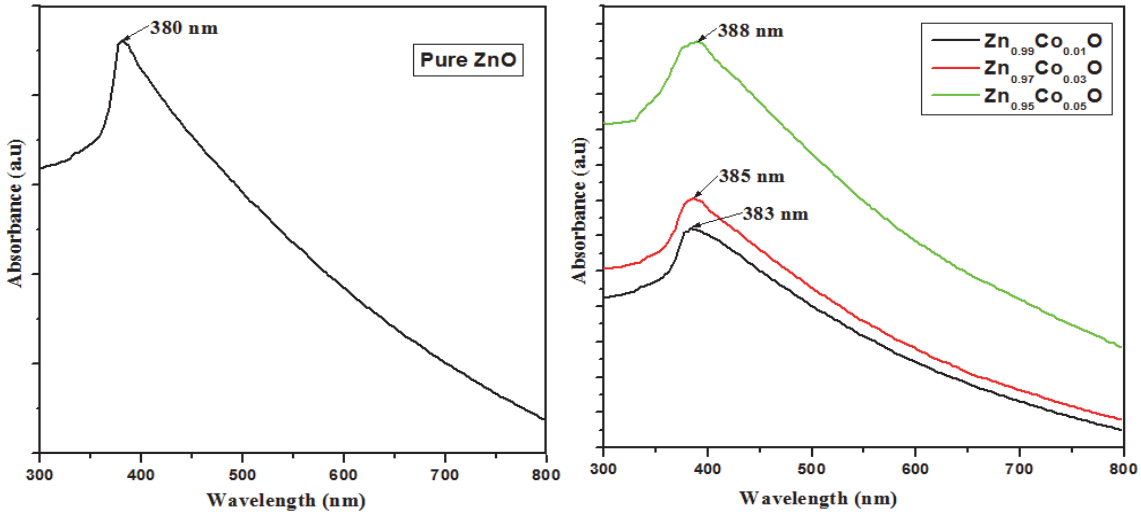

(a) **(b)**

Fig. 4: UV-Visible absorption spectra of the (a) undoped ZnO nanoparticles (b) Co-doped ZnO nanoparticles

4.4 Vibrating Sample Magnetometer (VSM) Analysis

All the measurements were made at room temperature. Pure ZnO sample shows no hysteresis curve as observed from figure 5 (a), confirmed the diamagnetic property. Diamagnetic nature of pure ZnO has also been reported in literature [27]. Whereas, from the magnetic hysteresis loops (shown in figure 5 (b-d)) for Co doped samples i.e. $Zn_{1-x}Co_xO$ (x=0.01, 0.03 and 0.05), it is clear that all samples exhibit hard ferromagnetic behavior at room temperature. The diamagnetic component was subtracted from the original data in order to determine the ferromagnetic part. The values of magnetic remanence (Mr) and coercivity (Hc) of our Co doped ZnO samples are shown in the table 3. It can be observed that coercivity (Hc) increases and remanence decreases with the increase in Co doping. These results are in contrast, as some researchers observed ferromagnetism (low coercivity value) only at lower doping concentration but paramagnetic behavior for higher doping concentration [22].

The Possibility of observed ferromagnetic behavior in our samples due to formation of metallic clusters or any other secondary phases is ruled out as no Co related oxides such as CoO and Co_2O_3 or Co cluster was observed from the XRD and EDX reports. Therefore, we can conclude that the presence of ferromagnetic behavior in our samples is due to intrinsic coupling between the atoms of doped materials and not due to the presence of metallic cluster or secondary phase (segregation).

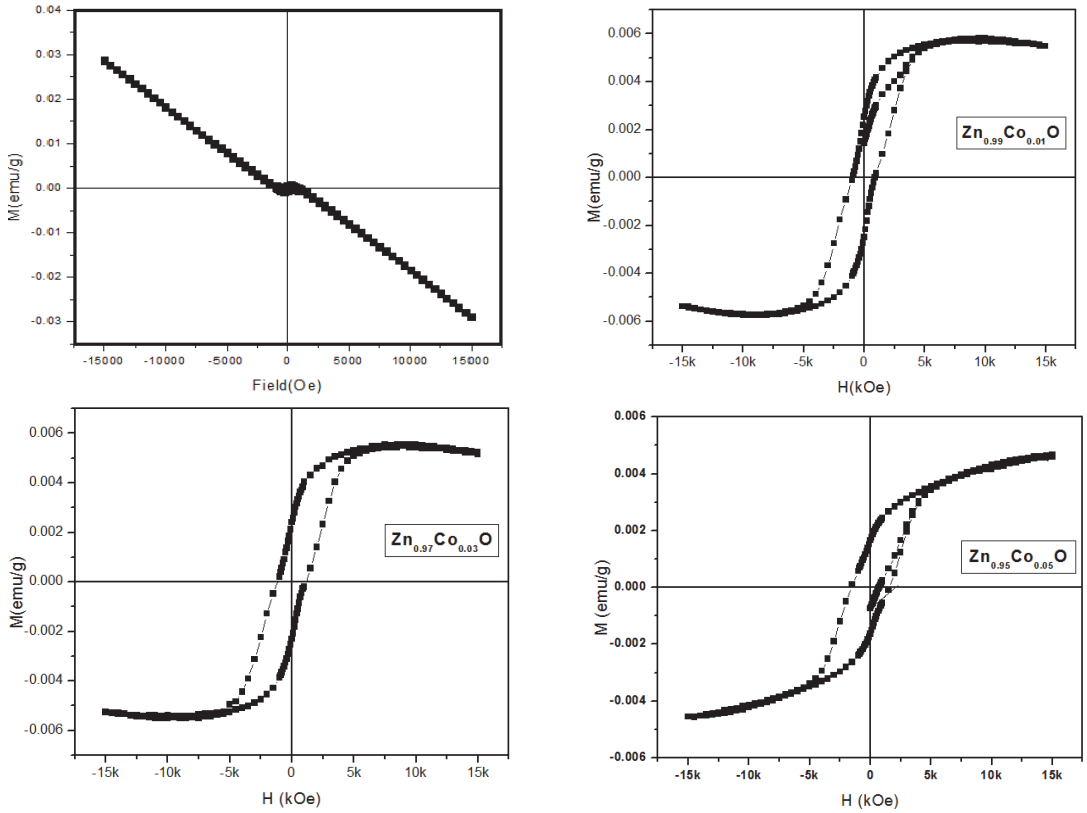

Fig. 5: Room temperature ferromagnetism of (a) Pure ZnO and (b-d) Co-doped nanoparticles

Table 3: Magnetic properties of $Zn_{1-x}Co_xO$ (x=0.01, 0.03 and 0.05) nanoparticles

Sample	Hc (Oe)	Mr (emu/g)
$Zn_{0.99}Co_{0.01}O$	897	2.49×10^{-3}
$Zn_{0.97}Co_{0.03}O$	1138	2.32×10^{-3}
$Zn_{0.95}Co_{0.05}O$	1566	**4.64 10^{-3}**

5. Conclusion

In this study, Co doped ZnO ($Zn_{1-x}Co_xO$ (x=0.01, 0.03 and 0.05)) diluted magnetic semiconductor nanoparticles were successfully synthesized via simple co-precipitation method. X-Ray diffraction pattern show formation of hexagonal wurtzite structure for all samples of Co doped ZnO. All the samples of $Zn_{1-x}Co_xO$ (x=0.01, 0.03 and 0.05) show room temperature ferromagnetic behavior as observed from the M-H curves. High value of coercivity in our samples confirmed formation of hard ferromagnetic material. A detailed analysis of XRD and EDX measurements revealed that the observed ferromagnetism is an intrinsic property of the material.

References

[1] R. Slama, F. Gharibi, A. Houas, C, Barthou, L. El Mir, Int. J. Nanoelectronics and Materials **3** (2010) 133.

[2] Ali A. Yousif, Adawiya J. Haidar, Nadir F. Habubi, Int. J. Nanoelectronics and Materials **5** (2012) 47.

[3] Evan T. Salem, Makram. A. Fakhri, Hala Hasan, Int. J. Nanoelectronics and Materials, **6** (2013) 121.

[4] T. Dietl, H. Ohno, F. Matsukura, J. Cibert, D. Ferrand. Zener, Science **287** (2000) 1019.

[5] S. A. Wolf, D. D. Awschalom, R. A. Buhrman, J. M. Daughton, S. Von Molnar, M. L. Roukes, A. Y. Chichel- kanova, D. M. Treger, Science **294** (2001) 1488.

[6] H. Ohno, Science **281**(1998) 951.

[7] G. A. Prinz, Science **282** (1998) 1660.

[8] S. Ghosh, K. Mandal, Journal of Magnetism and Magnetic Materials **322** (14) (2010) 1979.

[9] J. M. Wesselinowa, A. T. Aposto, Journal of Applied Physics **107** (5) (2010).

[10] D. Karmakar, S. K. Mandal, R. M. Kadam, P. L. Paulose, A. K. Rajarajan, T. K. Nath, A. K. Das, I. Dasgupta, G. P. Das, Physical Review B**75** (14) (2007).

[11] J. Luo, J. K. Liang, Q. L. Liu, F. S. Liu, Y. Zhang, B. J. Sun, G. H. Rao, Journal of Applied Physics **97** (8) (2005) 086106

[12] J. B. Wang, G. J. Huang, X. L. Zhong, L. Z. Sun, Y. C. Zhou, E. H. Liu, Appled Physics Letters **88**(25) (2006) 252502.

[13] O. D. Jayakumar, I. K. Gopalakrishnan, C. Sudakar, R. M. Kadam, S. K. Kulshreshtha, Journal of Crystal Growth **300**(2) (2007) 358.

[14] R. Elilarassi, G. Chandrasekaran, American Journal of Materials Science **2**(1) (2012) 46.

[15] G. J. Huang, J. B. Wang, X. L. Zhong, G. C. Zhou, H. L. Yan, Journal of Material Science **42** (2007) 6464.

[16] Sarvari Khatoon, Tokeer Ahmad, Journal of Materials Science and Engineering B2 **(6)** (2012) 325.

[17] V. K. Sharma, M. Najim, G. D. Varma, Adv. Mat. Lett. **3** (2) (2012) 107.

[18] Javier Blasco, Fernando Bartolome, Luis M. Garcia, Joaquin Garcia, J. Mater. Chem. **16** (2006) 2282.

[19] B. Martínez, F. Sandiumenge, Ll. Balcells, J. Arbiol, F. Sibieude, C. Monty, Applied Physics Letters **86** (2005) 103113.

[20] P. Bappaditya, P. K. Giri, International Journal of Nanoscience, **10** (1) (2011) 1.

[21] B. Martínez, F. Sandiumenge, Ll. Balcells, J. Arbiol, F. Sibieude, C. Monty, Physical Review B**72** (2005) 165202.

[22] Muhammad Ahsan Shafique, Saqlain A Shah, Muhammad Nafees, Khalid Rasheed, Riaz Ahmad, International Nano Letters **2:31** (2012).

[23] A. Faheem, K. Shalendra, A. Nishati, M.S. Anwar, Si Nae Heo, Bon Heun Koo, Acta Materialia **60** (13-14) (2012) 5190.

[24] Shalendra Kumar, Y. J. Kim, B. H. Koo, Heekyu Choi, C. G. Lee, Journal of the Korean Physical Society **55** (3) (2009) 1060.

[25] L. W. Yang, X. L. Wu, T. Qiu, Journal of Applied Physics **99** (2006) 074303.

[26] H. Zhang, D. Yang, S. Li, X. Ma, Y. Ji, D. Qu, Mater. Lett. **59** (2005) 1696.

[27] Y. Z. You, T. Fukumura, Z. Jin, K. Hasegawa, M. Kawasaki, P. Ahmet, T. Chikyow, H. Koinuma, J. Appl. Phys. **90** (2001) 4246.